Optimization of a Real Scale Shrouded Wind Turbine Using 3D CFD Analysis

Hoda Parsa*, Negin Maftouni**‡

*MSc Student at Department of Mechanical Engineering, Faculty of Engineering, Alzahra University, Tehran, Iran
**Faculty Member at Department Mechanical Engineering, Faculty of Engineering, Alzahra University, Tehran, Iran.
‡
Corresponding author email: n.maftouni@alzahra.ac.ir; Tel: +982185692141

Received: 08.05.2020 Accepted: 14.06.2020

ABSTRACT- This study aims to simulate and compare three different wind turbines; flanged shrouded wind turbine, shrouded turbine with no flange, and bared wind machine. The 3D models of all of the mentioned turbines are made. Velocity is the most effective parameter when studying output power. So in the present work, velocity is improved implementing different geometries. The outcomes indicate that among the three types, the maximum output power is made by the turbine, including a shroud and also an attached flange. The benefits of flanged shrouded wind turbines are discussed. The results report that when comparing with that of the bared wind turbine, output power rose by 106% with the use of a simple shroud and by approximately 137% with the use of a flange attached to the shroud. This improvement is the result of the occurrence of the low-pressure region at the shroud outlet, which is enhanced the presence of the flange in the best model. Low pressure leads to higher mass flow and consequently, higher power generation.

Keywords Wind energy, CFD, Optimization, Shrouded wind turbine, Ducted wind turbine.

1. Introduction

According to rising concerns about growing energy requirements and simultaneous climate's changes, the development of renewable energy resources has obtained great interest. Wind is one of the relevant examples. The traditional tools for extracting energy from wind are turbines. According to the principles of conservation of momentum and mass, the efficiency of all traditional wind turbines cannot be more than the Betz limit because of limitations on the optimum efficiency, as a result of parameters such losses of vortex in tip, drag force, and losses of wake. When a wind turbine is implemented to harvest the energy of wind, the extractable wind energy has a strong relationship with the speed of wind [1-5]. So a little rise in wind speed results in a notable increase in the harvested energy. There are some several research focused on novel and applicable approaches to raise the speed of the wind when contacting the turbine [6, 7]. Some researchers have suggested encasing wind machine in a shroud. More than increasing the speed of approaching wind, using a shroud reduces cut-in speed and consequently increases the total working time of the turbine. The shroud makes a low-pressure area at the outlet. The mentioned low-pressure region needs more mass flow to make up the negative pressure. In the case of presence of a flange at the end edge of the diffuser, the resulting vortex leads to even lower-pressure and higher mass flow and consequently, higher power output. One of the modern wind turbine machines is the diffuser-augmented wind turbine (DAWT), initially designed by two scientists, Lilley et al., in 1956 [8]. Consequently, experimental models of the concept were developed by researchers including Oman et al. [9], Igra [10, 11], Foreman and Gilbert [12], and Phillips et al. [13]. The experimental results of these works indicated that DAWTs could generate more wind energy than all the traditional wind turbines of identical rotor diameters. Hence, there are numerical and theoretical studies attempting to analyse as well as modify the efficiencies of DAWTs [14–18]. The results of Hasen's research indicated that the coefficient of power for the wing-profiled shrouded wind turbine is about 80% more than that of a similar traditional wind machine [14]. Van Bussel identified two power coefficients: one relevant to the rotor swept region, and the other related to the diffuser exit region [15]. The results showed that in most DAWTs, the power coefficients related to the shroud exit area are lower than the Betz coefficient, but those related to the rotor swept area exceed the Betz limit.

Computational fluid dynamics (CFD) is a useful analytical mean that has been used for a shroud wind machine with a plain duct by Jafari et al. [16]. The study reported that the performance of ducted machine had a magnitude near 70% greater than those of similar classic turbines. Using a shrouded model, Werle and Presz reported an increase of approximately 80% in thrust with medium pressures related to exit and diffusion plane [17]. In 2009, Jamieson reported that the best

thinkable optimum power coefficient of a DAWT related to the area of rotor swept is 8/9, that is 50% greater than the Betz limit [18]. Furthermore, Ohya et al. designed an innovative shrouded machine with a big flange on the diffuser end and an inlet section with a curved profile [19, 20]. The results of wind tunnel tests showed that a low-pressure region created by the big flange due the significant vortices made at the rear of the flange, thereby increasing the amount of wind entering the diffuser when compared with that in a normal DAWT without a flange. The numerical and experimental results indicated that mounting the flange raised the wind speed in the nozzle section of the shroud by about 60–140% in comparison with the upwind speed, and by about 20–70% in comparison with the velocity of wind in the nozzle section of a diffuser without any mounting flange. The aforementioned increase in wind velocity augmented the power extracted by about 100–200% in comparison with that of a traditional wind turbine, and by 40–110% in comparison with a turbine with the same shroud but no brim. In 2008, Ohya demonstrated that the power generated by a 0.5 kW shrouded machine integrated with a long brimmed was about 300-400% more, comparing with that of a classic bared turbine with identical rotor dimensions [21]. In another study, the effect of a flange-attached shroud on the dynamics of the running blades of a 3 kW wind turbine was studied using wind tunnel tests [22]. The results revealed an increase of about 35% in the rotational velocity of blades in the flanged model. The greater the rotational speed, the higher were the strains at the roots of the rotating blades. Related theories were modified by Khamlaj and Rumpfkeil, and the 1D system derived was suitable for providing good approximations of the performances of shrouded devices at the beginning of the design stage [23]. Mansour et al. performed a numerical analysis of ducted wind turbines, and the results indicated that the shape of the shroud affects performance [24].

Flanged diffusers were used in another study, and the tests showed that a 5 kW flanged shrouded wind turbine gained about 2.5 times rise in output power in comparison with the bared wind turbine [25]. Earlier, it was indicated that the power coefficient of a DAWT (0.54) is higher than that of a traditional wind turbine without a shroud (0.4). A new research performed by Takahashi et al. indicated that shrouded turbines have another notable benefit of noise reduction [22]. The usual vortices from the interactions of blade tips with wind flow are damped in this design. Hence, it can be concluded that shrouded wind turbines are more suitable for installation near urban areas. It is noteworthy that the rotor diameters considered in some of these studies were 0.088 m [10], 0.045 m [12], 7.3 m [15], 4 m [26], and 0.5 m [27].

Recently a research group performed a combination of experimental and numerical studies for a new design including a small twin-rotor wind turbine combined with shroud. The numerical analysis of the time-averaged FRM flow fields reported that the presence of the second rotor might reduce the mass flow rate of the upstream turbine, especially when the downstream rotor is placed near to the diffuser inlet [28, 29].

In 2020, Leloudas et al. worked on a methodology for the design optimization of small diffuser augmented wind turbine shrouds. Their proposed a methodology that was applied to the aerodynamic shape optimization of an axisymmetric shroud for a 15 kW diffuser augmented wind turbine, aiming to maximize the mean velocity speed-up ratio and minimize drag force, while maintaining the throat diameter of the baseline shroud design; a geometrical constraint ensuring that the volume of the optimal design will be less or equal to the volume of the baseline one, was also imposed [30].

None of the past performed research has considered a large shrouded wind turbine for neither experimental nor numerical studies. Also, in most of the past numerical research, a section technique has been implemented to reduce the computational cost [16, 30]. Besides there is no comparative study including all three cases of bared wind turbine, simple shrouded wind turbine and flanged shrouded wind turbine. In The current study the focuse is on juxtaposition of the outputs of the three various systems in the power subject, and also on getting the most efficient model. Here a comparative study is performed on a set of three wind turbines including a shrouded wind turbine with a flange, a bared turbine and a flangeless shrouded one with identical dimensions. For the first time, the analyzed turbine is of a typical applicable large dimension and has a 30 m swept area diameter. Further, the entire system has been simulated without any use of similarity section technique, consequently resulting in achievement of more accurate outcomes. Finally, due to advantages of new light and strong materials, a long shroud has been included to improve the system.

2. Methods and Materials

In this part, three sessions are explained; theory of wind turbines, diffuser development, and CFD simulation. Before starting, the flow-chart of simulation is showed in figure 1.

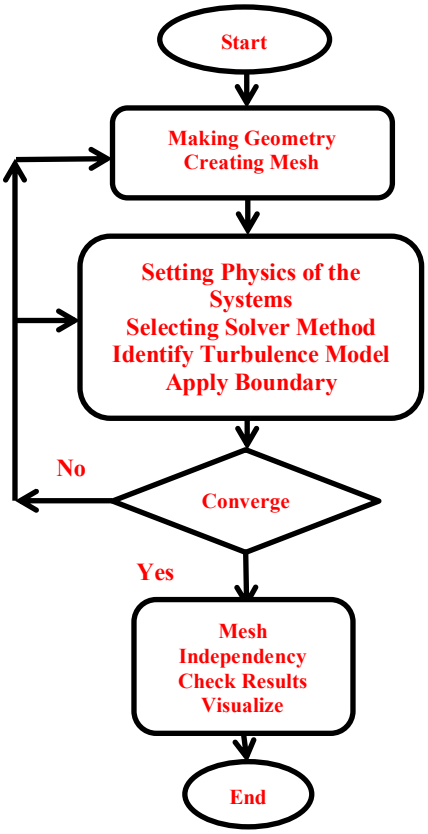

Fig. 1. Flow-chart of CFD simulation in this study.

2.1. Theory of Wind Turbines

The Betz coefficient is used like a criterion for comparing various kinds of wind machines. The following expressions explain the relations between multiple parameters. Figure 2 shows the geometry [31].

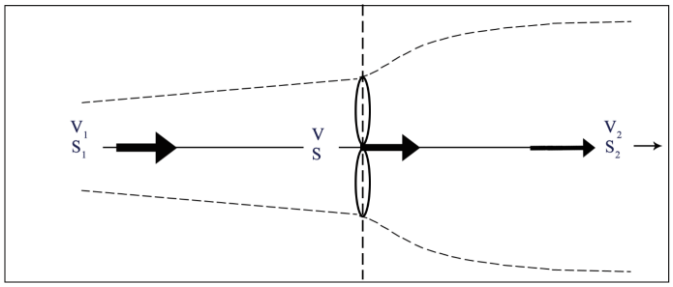

Fig. 2. The position of the parameters in the schematic of the wind around a turbine.

The total kinetic power is gotten from Equation 1.

$$W = \frac{1}{2}\rho S V^3 \quad (1)$$

Due to the shape illustrated in Figure 1, an annular tube of airflow is considered to explain the extractable power.

$$P = \rho S V^2 . (V_1 - V_2) \quad (2)$$

The factor of downstream velocity, "a", is expressed as the ratio of downstream velocity V_2 to upstream velocity V_1.

$$a = \frac{V_2}{V_1} \quad (3)$$

The performance coefficient, "C_p", is the ratio of the harvestable power to the entire kinetic energy W of the undisturbed flow.

$$C_p = \frac{P}{W} = \frac{T\omega}{W} \quad (4)$$

Another way results in exact outcomes by putting the rotor area, $S = 3/2\ S_1$.

$$P_{ideal} = \frac{16}{27}\frac{1}{2}\rho S {V_1}^3 \quad (5)$$

The Betz limit shows that in the best situations a wind turbine may harvest 59.3% of the wind energy.

$$Betz\ coefficient = \frac{16}{27} = 59.3\ \% \quad (6)$$

Taking in count the roughness of the blade surface, mechanical imperfections, and frictional losses, about 30–42% of the energy included in the wind is usually harvestable.

$$Betz\ Equation = P_{max} = \frac{16}{27}\frac{1}{2}\rho {V_1}^3 \frac{\pi D^2}{4} \quad (7)$$

The Betz limit indicates that a change in the wind velocity between downstream and upstream is needed to extract the power of the wind [26].

2.2. Diffuser Development

Different types of diffusers may be candidates as a part of shrouded wind machines. The most significant parameters when designing a diffuser are angle and length. Also, the design of the flange is important. Two types of systems usually are developed, long shroud and short shroud. Using a long type shroud leads to more wind speed acceleration near the inlet of the shroud. Regarding to new modern materials, the problem Figure 3 shows a long diffuser.

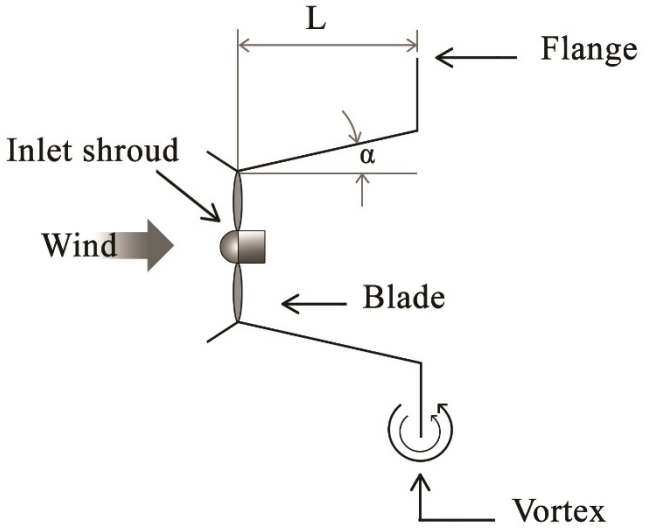

Fig. 3. A wind turbine with a long shroud.

External air, including high energy is injected to the wall of the shroud and leads to an additional axial momentum in the boundary layer. This momentum weakens the adverse pressure and reduces the probability of flow separation. Past works have indicated the positive points of long diffusers [21, 27].

In the current research, the shrouded and simple bare turbines were of equal blade diameters.

2.3. CFD Simulation

In this study, a shrouded wind turbine and its bare counterpart were modeled and analyzed separately. The process entailed the following steps: building the 3D model, meshing it, establishing design parameters, and the solution stage. The results were then extracted and analyzed. The 3D models were then created, and the effects of shroud on velocity and pressure distribution, produced momentum, and power performances were studied.

2.3.1. Design of 3D Model

For the first step, 3D models of all kinds of turbines were constructed, as shown in figure 4.

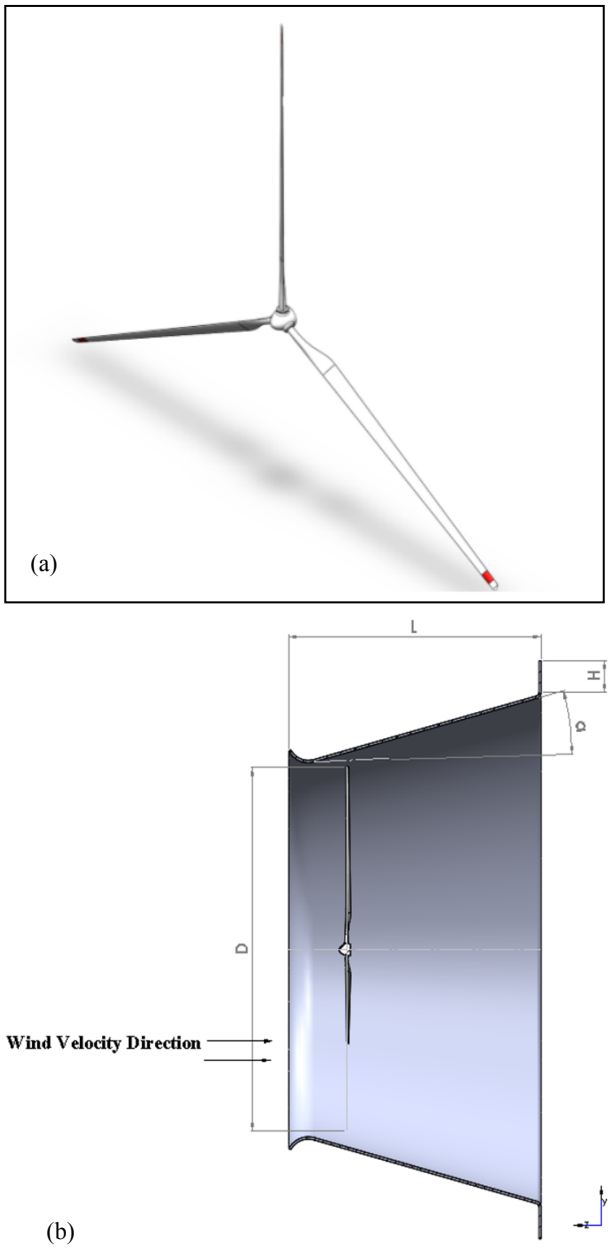

Fig. 4. Turbines structure models (a) Bared turbine (b) Dimensions of Shrouded machine.

A symmetric NACA0012 airfoil with a chord of 0.75 m was considered in these wind turbines' blades design as is shown in figure 5. Besides, the sharp edges of hub-blade connection were replaced with curvatures to satisfy numerical calculation requirements.

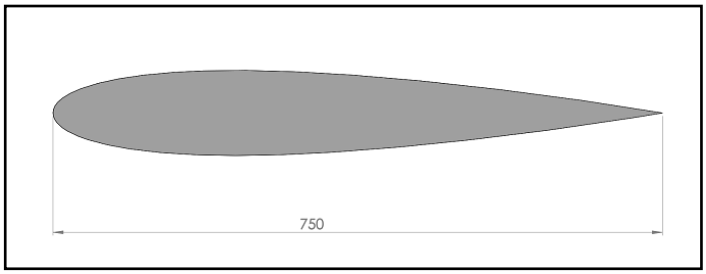

Fig. 5. The shape of NACA0012.

Design parameters of all three types are described in Table 1. The angle of diffuser is selected due to criterion proposed in [16]. The swept area is 707 m^2, the nominal power of the bared wind turbine is 85.85 Kw, its cut in velocity is 2 $m.s^{-1}$ and its cut off velocity is 25 $m.s^{-1}$. The blades are made of composite.

Table 1. Design parameters of the different wind turbines.

	Diameter (D)	**Length (L)**	**Angle**	**Flanged (m)**
Wind Turbine	30 m	-	-	-
Simple Shrouded	31 m	30 m	15°	-
Flanged Shrouded	31 m	30 m	15°	2

2.3.2. Mesh

To make a strong mesh for the model is one of the crucial steps affecting solution accuracy in CFD methods. A tetrahedral mesh was considered to construct the grid. The mesh around the blades may be observed in figure 6.

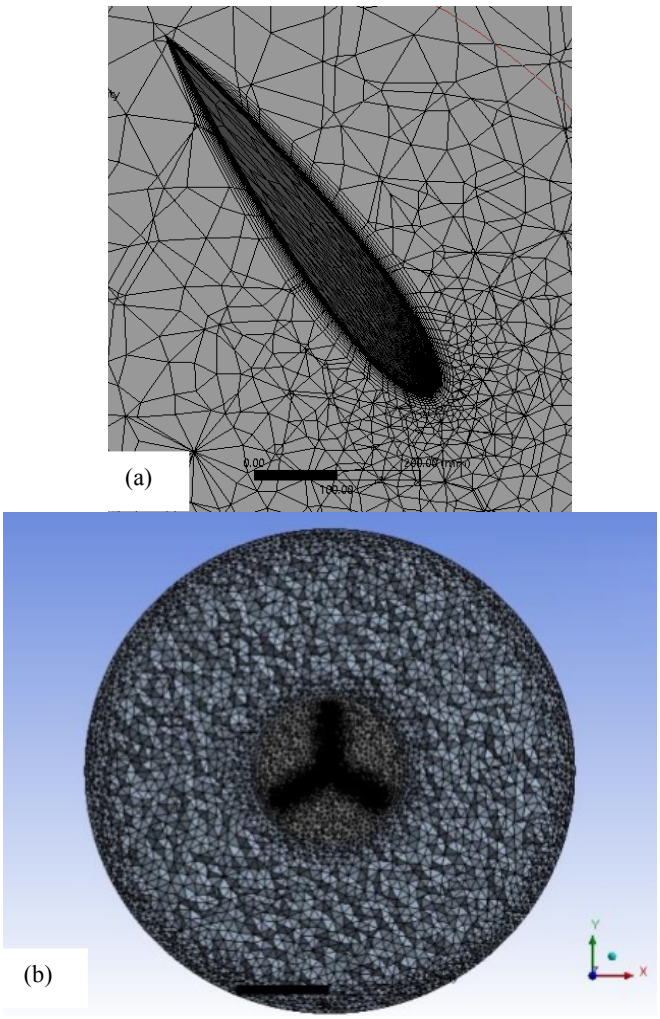

Fig. 6. Mesh modeling (a) Front view, (b) Boundary Layer around the Blade.

The space here had two regions: motion frame part and the area that air had movements and affected blades behaviour. Figure 7 shows these two sections.

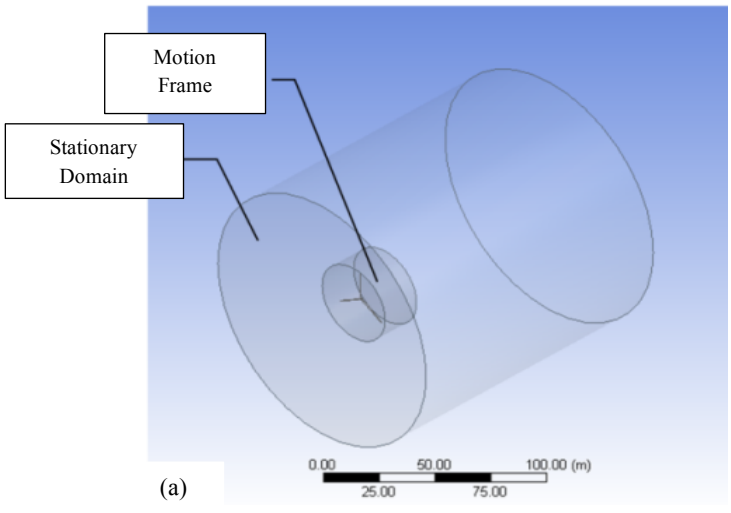

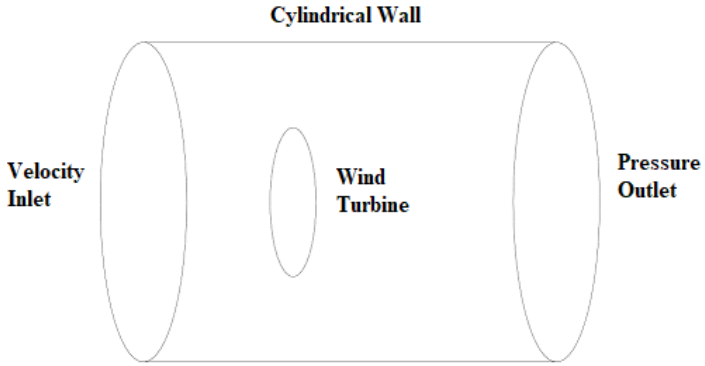

I (b) ı) Motion frame and stationary domain, (b) Boundaries for the simulation domains in CFD.

A fine curvature was made in the motion frame. Although it is hard to produce high-quality solving meshes in these dimensions, some various mesh were generated to study mesh-independency. The results indicated that the momentum versus approaching wind velocity remained almost constant for grids with 25,157,435 or more cells. Hence, to save computation time, the grid with 25,157,435 cells was selected.

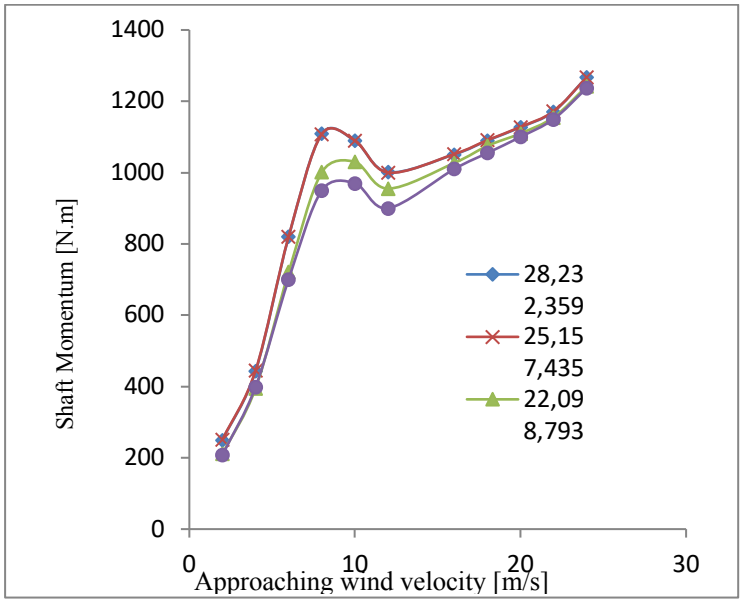

Fig. 8. Mesh-independency study for momentum results of 4 different meshes.

The boundary layer was implemented near the external surface of the blades to improve the level of calculations. The small direct lines in Figure 5 show the boundary layer

region. A total of 25 layers were considered in the boundary layer to solve, and the first of these layers was at a distance of 0.04 mm from the wall. In this situation, there was an interval shorter than y^+=10 between the wall and its first grid node in the direction perpendicular to the wall. The non-dimensional inter-spaces from the wall usually useful in studying a turbulent boundary layer was named y^+ (ρU_f y/μ). The magnitude of y^+ at the first grid point near the wall must be lower than 10 for the viscous sublayer and phenomenon of separation to be considered correctly [32]. The value of y^+ in the present research was obtained, and the result is reported in Figure 9. The highest calculated magnitude of y^+ was less than 10, and the design criterion was satisfied.

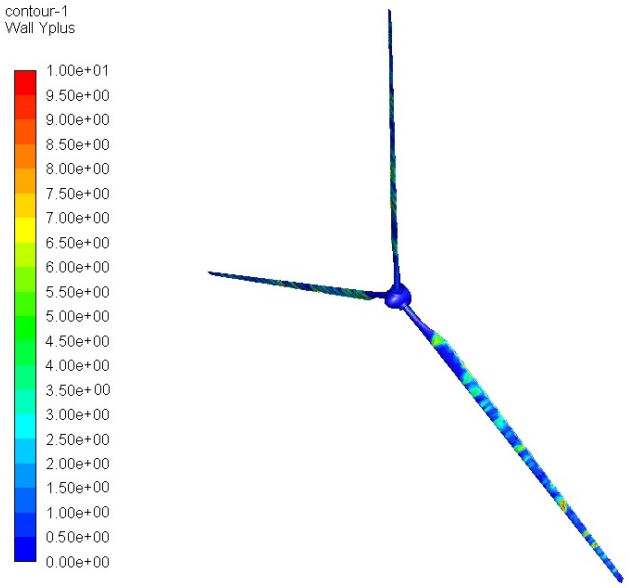

Fig. 9. Wall Y+ values of the blades in this solution.

Furthermore, the average value of Skewness is 0.25, and its maximum value was 0.98, that both parameters were acceptable [33].

2.3.3. Boundary Conditions and Turbulence Model

In this study, the problem was considered in steady-state. The multiple reference frames (MRF) model was implemented. Frame motion is a steady-state approach. The rotating part here was the wind machine with the disk around it. A velocity of 2 rad.s^{-1} was considered for the MRF, in all cases. The most preferred range for ƛ is (3–5), and the tip speed ratio ƛ was considered to be 3.750 [16]. The next section in the grid is the stationary part. The speed at entrance was deemed to be 8.0 m.s^{-1} and the outlet BC was the zero relative pressure. The external wall was considered symmetric. The region between the air tunnel and the MRF was considered as a wall with the no-slip condition. For all of the walls, the no-slip BC was assumed. The standard pressure correction method and a first-order upwind model were implemented.

The shear-stress transport (SST) model was then applied. This model is based on Bradshaw's hypothesis that the main shear-stress is commensurate with the turbulent kinetic energy. This model has been tested for various flow fields. This model predicts results independent of the free stream volumes [34].

The performance of the shroud is influenced by the phenomenon of separation. Hence, one of the most essential steps in solving a problem with CFD simulation is to choose a proper model that can forecast the separation precisely. In the case of 2D separation in Reynolds-averaged Navier–Stokes (RANS), the SST model has been studied deeply [35]. In another research, the SST, seven-equation Reynolds stress model, v^2–f, and low-Reynolds k–ε models were compared [36]. The best forecast for separation was obtained from the v^2–f model. This model is a modified SST k–ω RANS model [16].

SST k–ω model was implemented in the current study. The time step was 1E-04, and the solution was allowed to run and converge reaching to a consistent/stable state while achieving a low level of different residuals at each time step.

3. Results and Discussion

The pressure and velocity diagrams of the simple bared turbine are represented in figure 10.

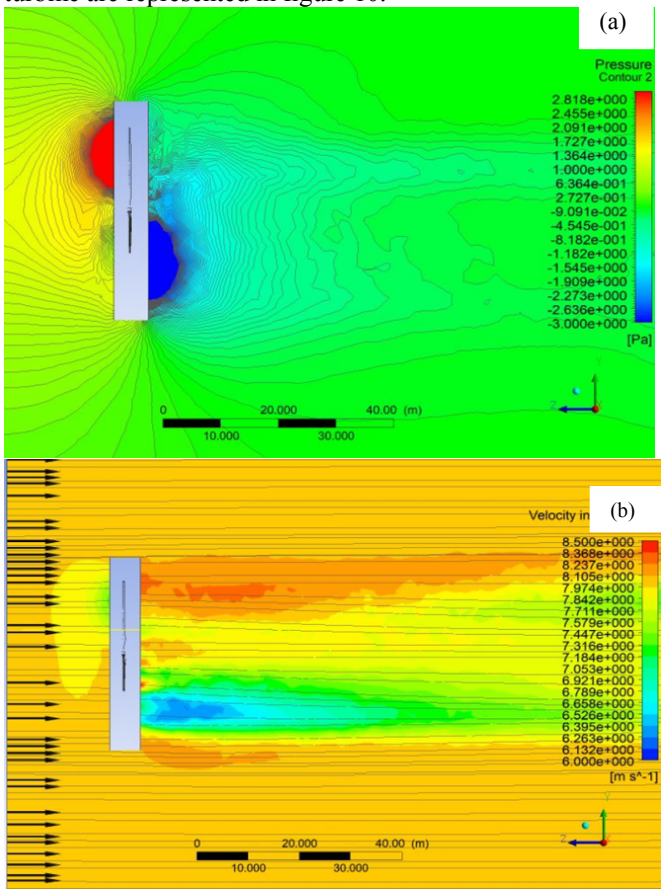

Fig. 10. Simple bared Turbine (a) Pressure diagram (b) Speed diagram in YZ.

Also for the simple shrouded and flanged shrouded wind turbines, similar diagrams are shown in figures 11 and 12, respectively.

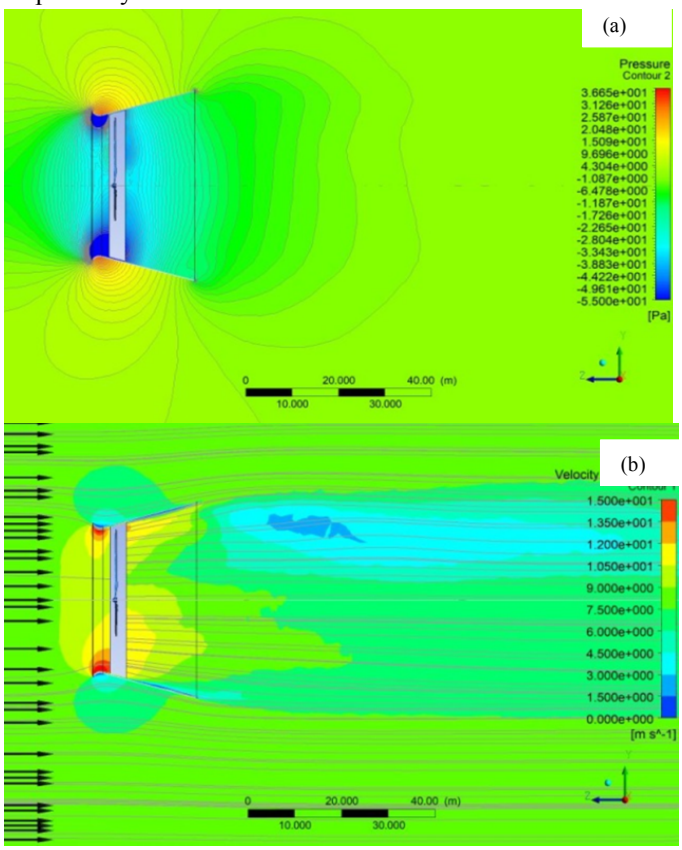

Fig. 11. Simple shrouded turbine (a) Pressure diagram in YZ, (b) Speed distribution in YZ.

The YZ plane is normal to the rotor region. So the result of wind experiencing the blades is apparent there. As it is shown in Figures 10-12, uniform speed diffusion has occurred and may be seen.

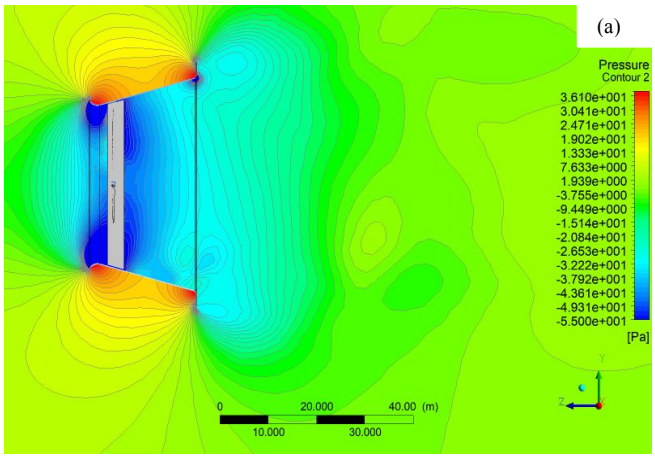

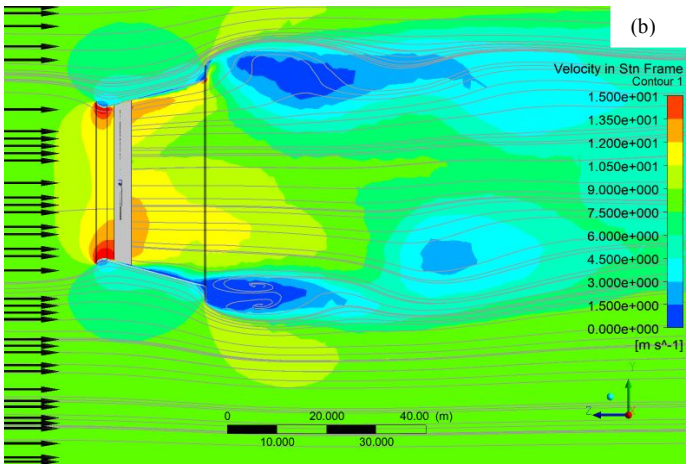

Fig. 12. Flanged Shrouded Turbine (a) Pressure diagram in YZ, (b) Speed diagram in YZ.

It can be observed that the streamlines flowed moderately inside the diffuser and exactly after. Also, the speed didn't reduce in the shroud as it was predicted to make up the pressure drop at the end of the shroud. The uniform distribution of speed was more obvious in the shrouded case than in the bared one. It is evident considering figures 11 and 12, that the speed increases from 8.0 m s^{-1} to near 12.0 m.s^{-1} in the place that wind approaches the turbine. In the bared turbine, this rise in speed was not observed (Figure 10).

Down stream, the flow was expanded in the shroud. So the a pressure drop was seen at the outlet of the shroud and an increase of the mass flow was observed at the inlet of the shroud. As a result, more lift force was made on the blades, leading to a drop in pressure beyond the wind machine on the suction region.

This phenomenon resulted in the higher performance of the turbine with a rise in flow rate, as described in previous sections. The reduction in pressure is higher in the case of the flanged turbine. The pressure decrease after the turbine is approximately 53 Pa for the shrouded wind turbines. Still, in the flanged turbine, a broader region experiences lower pressure than in the shrouded wind turbine without flange, according to figures 11 and 12. In the bare turbine, the pressure decrease after the blades is just about 3 Pa as it is observable in figure 10. Vortex formation behind the brim leads to higher mass flow to the turbine inside the shroud, thereby causing a broader low-pressure region and finally increasing power output. The momentum is calculated in all the cases and is presented in table 2. The maximum momentum was observed in the flanged shrouded wind turbine.

Table 2. The momentum of the different Wind Turbines.

	Bare Wind Turbine	Simple Shrouded Wind Turbine	Flanged Shrouded Wind Turbine
Momentum [N.m]	1062	1068	1108

Figure 13 compares the pressure coefficient of the different kinds of wind turbines designed with the parameters presented in Table 1.

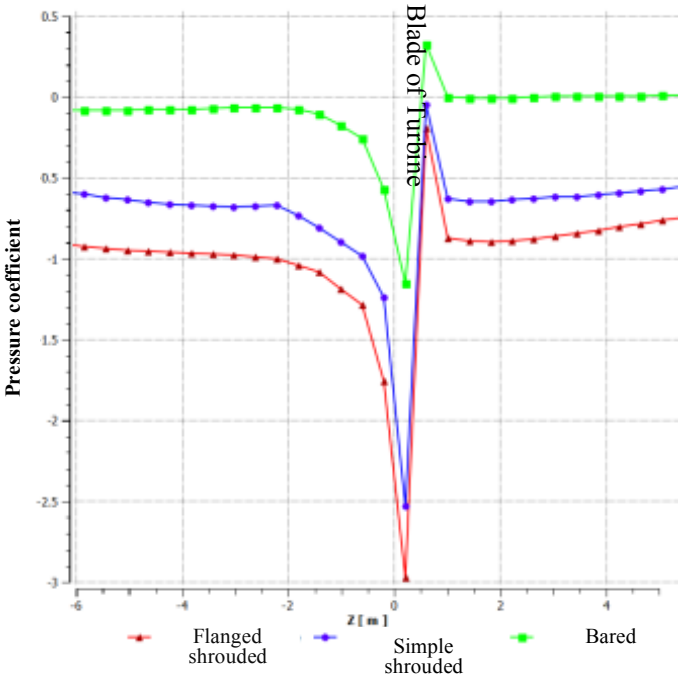

Fig. 13. Pressure coefficient distributions for three types of studied cases.

In all of the analyzed systems, the most significant reductions in the pressure coefficient were made after the machine. The outcomes had a reductive trend in total pressure exactly after the turbines. The ducted turbine, including a flange resulted in the presence of a more strong pressure gradient, and as a consequent, more flow rate and output power and the bared case showed a lower value at all. These points had acceptable compatibility with figures 8a, 9a, and 10a.

Figure 14 reports the output power for all various systems. Figure 14 shows that the extracted power has improved near to 106% after including a simple shroud in the system, and by about 137% when a flange was also added.

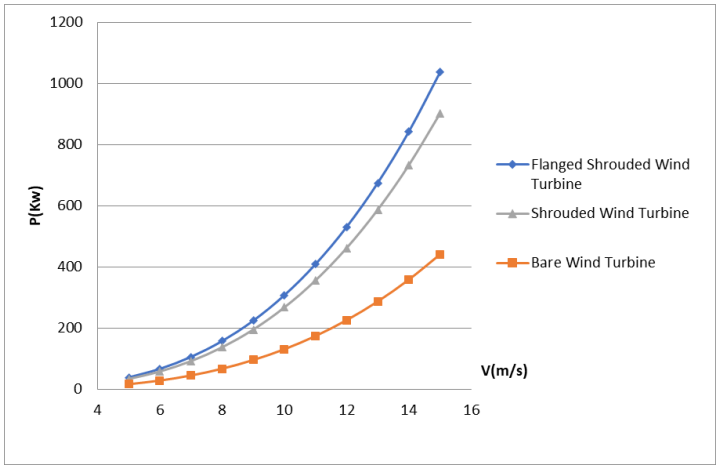

Fig. 14. The power output of all turbine types, versus wind speed. (*Cp*= 0.68 for the flanged shrouded type).

This result looks the same for all speeds. The maximum generated power is 67.0 kW in the case of the bared machine, 137.0 kW by the simple shrouded one, and 157.0 kW by the flanged shrouded case. The diameter of studied wind turbines was 30 m, and the average wind velocity was considered 8.0 $m.s^{-1}$, a generally available magnitude in Iran. This rise in the output power is compatible with the outcomes of past researches [16].

4.Validation

To validate the achieved results, the unsteady-state simulation was performed for the bared case. The output powers of two states of steady and unsteady were compared for different wind velocities to assess the error. All boundary conditions were considered the same. Figure 15 shows the validation results. It is obvious that the outcomes are very close

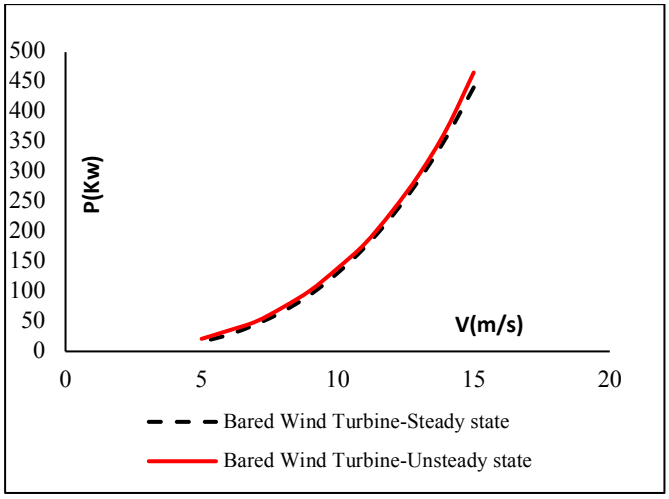

Fig. 15. Power of bared wind turbine for the steady and unsteady states versus wind velocity.

Also trend of the pressure diagram (figure 13) was in the same way of past reported results [27], and this was one of

the validating points in the present research. See figure 16 to compare.

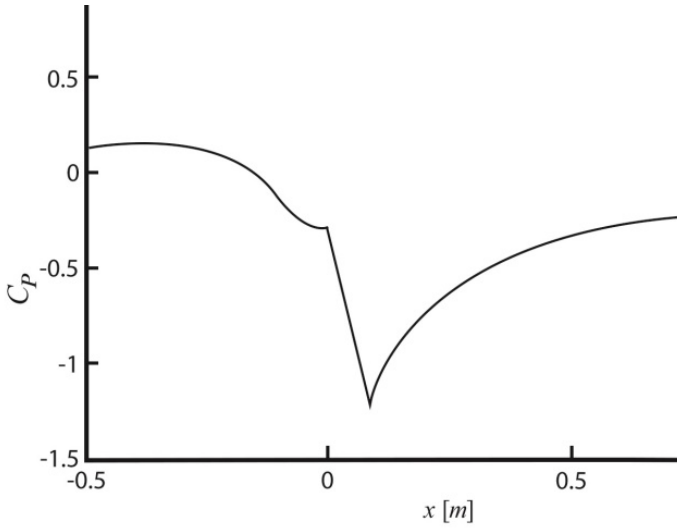

Fig. 16. Distributions of the pressure coefficient [27].

The lift and drag coefficients of NACA0012 were calculated and compared with experimental published results in the same Reynolds numbers in the common ranges [37]. Figures 17 and 18 show the comparative diagram.

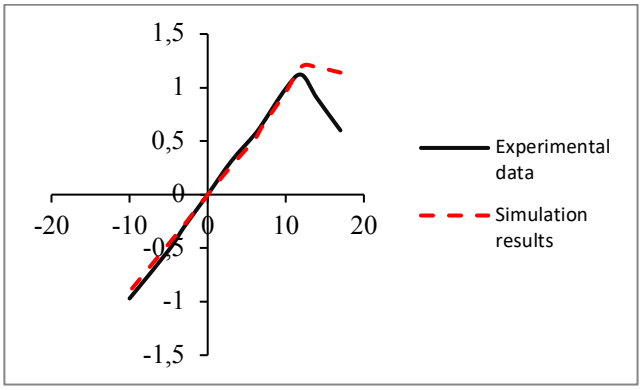

Fig. 17. Lift coefficient versus angle of attack for simulation and experimental results.

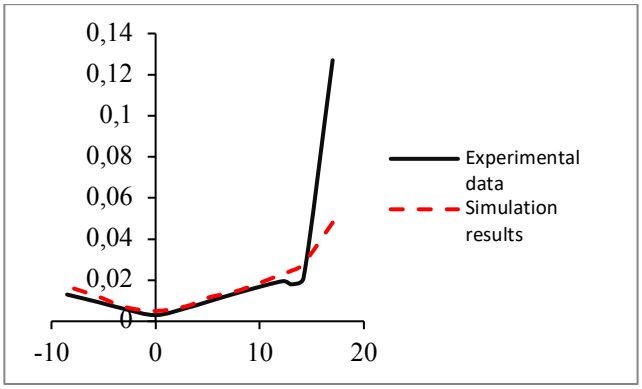

Fig. 18. Drag coefficient versus angle of attack for experimental [32] and current simulation results.

It is obvious that the simulation results are close enough to the experimental data for both of lift and drag coefficients.

5. Conclusion

Numerical analysis is done for three various types of wind turbines: bared, simple shrouded, and flanged shrouded models. The results show a similar trend with previous theoretical and experimental researches' reports in terms of power increase and also pressure and speed distributions trend. The outcomes show that the flanged shrouded wind turbine has the most performance among all analyzed cases. The special achievement of the present research is to study a large wind turbine with actual applicable size and also to study the total three dimensional CFD model with nosimilary section considered. The results indicate that incomparison with that of the bared wind turbine, output power increasesa by 106% with the use of a simple shroud and by approximately 137% with the use of a flange attached to the shroud. Hereupon this focus, the output of this study could be used in the manufacturing field and the calculation would be extended on the other parts of research, such as the strengthening of the future wind turbines structures. Computation demonstrates that available bared turbines could be changed with flanged shrouded types. Due to new modern stength and light weighted materials, the concerns about high weight of long shrouds are removing. In Iran, this novel models have not been made, and it is logical to study this wind turbine type experimentally.

References

[1] C. J. Crabtree, D. Zappala, and S. I. Hogg, "Wind energy: UK experiences and offshore operational challenges", Proceeding of IMechE Part A: Journal of Power and Energy. Vol. 229, No. 7, pp.727–746, 2015.

[2] A. Harrouz, I. Colak and K. Kayisli, "Energy Modeling Output of Wind System based on Wind Speed," *2019 8th International Conference on Renewable Energy Research and Applications (ICRERA)*, Brasov, Romania, 2019, pp. 63-68, doi: 10.1109/ICRERA47325.2019.8996525.

[3] E. Bekiroglu and M. D. Yazar, "Analysis of Grid Connected Wind Power System," 2019 8th International Conference on Renewable Energy Research and Applications (ICRERA), Brasov, Romania, 2019, pp. 869-873, doi: 10.1109/ICRERA47325.2019.8996528.

[4] K. Muto, N. Namura, Y. Ukei and N. Takeda, "Model-Based Load Estimation for Wind Turbine Blade with Kalman Filter," 2019 8th International Conference on Renewable Energy Research and Applications (ICRERA), Brasov, Romania, 2019, pp. 191-199, doi: 10.1109/ICRERA47325.2019.8997085.

[5] S. Ermis, M. Yesilbudak and R. Bayindir, "Optimal Power Flow Using Artificial Bee Colony, Wind Driven

Optimization and Gravitational Search Algorithms," 2019 8th International Conference on Renewable Energy Research and Applications (ICRERA), Brasov, Romania, 2019, pp. 963-967, doi: 10.1109/ICRERA47325.2019.8996559.

[6] A. Vardar, B. Eker, F. Kultulmus, and O. Taskin, "Developing wind concentrator systems for the use of wind turbines in areas with low-speed wind potentials", Energy Technology, Vol. 3, No. 12, pp. 1260-1270, 2015.

[7] E. Ertutk, "Preliminary Analysis of a Concept Wind Turbine Blade with Piecewise Constant Chord and Constant Twist Angle Using BEM Method", International Journal of Renewable Energy research (IJRER), Vol. 8, No. 4, pp. 1890-1902, 2018

[8] G. M., Lilley, and W. J. Rainbird, "A Preliminary Report on the Design and Performance of Ducted Windmills"; Report 102; College of Aeronautics Cranfield: Cranfield, UK, 1956.

[9] R.A. Oman, K.M. Foreman, and B.L. Gilbert, "A progress report on the diffuser augmented wind turbine. In Proceedings of the 3rd Biennial Conference and Workshop on Wind Energy Conversion Systems", Washington, DC, USA, pp. 829–826, 8–12 June, 1975.

[10] O. Igra, "Research and development for shrouded wind turbines." Energy Conversion Management, No. 21, pp.13–48, 1981.

[11] O. Igra, "Compact shrouds for wind turbines." Energy Conversion Management, No. 16, pp.149–157, 1977.

[12] K. M. Foreman, B. Gilbert, and R. A Oman, "Diffuser augmentation of wind turbines." Solar Energy, 20, pp. 305–311, 1978.

[13] D. G. Phillips, P. J. Richards, and R. G. J Flay, "CFD modeling and the development of the diffuser augmented wind turbine." Wind Structure, No. 5, pp. 267–276, 2002.

[14] M.O.L. Hansen, N.N. Sorensen, and R.G.J, Flay, "Effect of placing a diffuser around a wind turbine." Wind Energy, No. 13, pp. 207–213, 2002.

[15] G.J.W. Van Bussel, "The science of making more torque from wind: Diffuser experiments and theory revisited." J. Phys. Conf. Ser., 75, doi:10.1088/1742-6596/75/1/012010, 2007

[16] S.A.H. Jafari, B. Kosasih, "Flow analysis of shrouded small wind turbine with a simple frustum diffuser with computational fluid dynamics simulations." Journal of Wind Engineering and Industrial Aerodynamics, No. 125, pp.102–110, 2014.

[17] M.J. Werle, and W.M. Presz, "Ducted wind/water turbines and propellers revisited", Journal of Propulsion and Power, No. 24, pp.1146–1150, 2008.

[18] P.M. Jamieson, "Beating Betz: Energy Extraction Limits in a Constrained Flow Field." Journal of Solar Energy Engineering, Vol. 45, No. 3, pp. 131, 031008, 2009.

[19] Y. Ohya, T. Karasudani, A. Sakurai, and M. Inoue, "Development of high-performance wind turbine with a brimmed diffuser—Part 1", Journal of the japan society for aeronautical and space sciences, No. 50, pp.477–482, 2003.

[20] Y. Ohya, T. Karasudani, A. Sakurai, and M. Inoue, "Development of high-performance wind turbine with a brimmed diffuser—Part 2", Journal of the japan society for aeronautical and space sciences, No. 52, pp.210–213, 2004.

[21] Y. Ohya, T. Karasudani, A. Sakurai, and M. Inoue, "Development of a shrouded wind turbine with a flanged diffuser." Journal of Wind Engineering and IndustrialAerodynamics,https://doi.org/10.1016/j.jweia.2008.01.006, No. 96, pp. 524–539, 2008.

[22] S. Takahashi, Y. Hata, Y. Ohya, T. Karasudani, and T. Uchida, "Behavior of the blade tip vortices of a wind turbine equipped with a brimmed-diffuser shroud", Energies, Vol. 5, No. 12, pp. 5229-42, 2012.

[23] T.A. Khamlaj, and M. P. Rumpfkeil, "Theoretical analysis of shrouded horizontal axis wind turbines", Energies, Vol. 10, No. 38, pp. 19-32, 2017.

[24] K. Mansour, and P. Meskinkhoda, "Computational analysis of flow fields around flanged diffusers", Joournal of Wind Engineering and Industrial Aerodynamics, Vol. 124, pp. 109–120, 2014.

[25] Y. Ohya, and T. Karasudani, "A shrouded wind turbine generating high output power with wind-lens technology", Energies, No. 3, pp. 634–649, 2010.

[26] W.X., Wang, T. Matsubara, J. F. Hu, S. Odahara, T. Nagai, T. Karasutani, and Y. Ohya, "Experimental investigation into the influence of the flanged diffuser on the dynamic behavior of CFRP blade of a shrouded wind turbine", Renewable Energy, No. 78, pp. 386–397, 2015.

[27] T.A. Khamlaj, and M.P. Riumpfkeil "Analysis and optimization of ducted wind turbines", Energy Journal, DOI: 10.1016/j.energy.2018.08.106. Vol. 162, pp. 1234-1252, 2018.

[28] M. Lipian, I. Dobrev, F. Massouh and K. Jozwik, "Small wind turbine augmentation: Numerical

investigations of shrouded and twin-rotor wind turbines", Energy, https://doi.org/10.1016/j.energy.2020.117588, Vol. 201, June, 2020.

[29] M. Lipian, I. Dobrev, F. Massouh and K. Jozwik, "Small wind turbine augmentation: Experimental investigations of shrouded- and twin-rotor wind turbine systems", Energy, DOI : 10.1016/j.Energy.2019.115855, Vol. 186, Nov. 2019.

[30] S. N. Leloudas, G. N. Lygidakis, A. I. Eskantar, and I. K. Nikolos, "A robust methodology for the design optimization of diffuser augmented wind turbine shrouds", Renewable Energy, Vol. 150, issue C, pp. 722-742, 2020.

[31] Tim Ackerman, "Wind Power in Power Systems", Ed. J. Wiley and Sons, 2005.

[32] T. Yavuz, E. Koç, B. Kılkış, O. Erol, C. Balas, and T. Aydemir, "Performance analysis of the airfoil-slat arrangements for hydro and wind turbines applications" , Renewable Energy, No. 74, pp. 414-421, 2015.

[33] ANSYS FLUENT 12.0 User's Guide/Mesh Quality/Skewness.

[34] F. R. Menter, "Zonal 1993 "Two Equation k-ω Turbulence Models for Aerodynamics Flows." 24th Fluid Dynamics Conference, Orlando, Florida, pp. 1-21, 6-9 July, 1993.

[35] M. Shives, and C. Crawford, "Computational analysis of ducted turbine performance", Proceedings of the 3rd International Conference on Ocean Energy, Bilbao, 2010.

[36] S. M. El-Behery, M. H. Hamed, "A comparative study of turbulence models performance for separating flow in a planar asymmetric diffuser", Computational Fluids No. 44, pp. 248–257, 2011.

[37] E.C. Douvi, and D. P. Margaris. "Aerodynamics characteristics of S809 vs. NACA 0012 airfoil for wind turbine applications", 5th International Conference from Scientific Computing to Computational Engineering, Athens, 4-7 July 2016.